

A Study of transverse bowing defect in cold roll forming asymmetric corrugated channels

Chuntian Xu (✉ xuchuntian@163.com)

Liaoning Institute of Science and Technology

Jianchao Chen

Yifan Wei

Han Han

Xu Zong

Ye Yuan

Research Article

Keywords: Asymmetric corrugated channels, Transverse bowing defect, Cold roll forming, Simulation, Parameter effect

Posted Date: April 25th, 2022

DOI: <https://doi.org/10.21203/rs.3.rs-1563551/v1>

License: © ⓘ This work is licensed under a Creative Commons Attribution 4.0 International License.

[Read Full License](#)

A Study of transverse bowing defect in cold roll forming asymmetric corrugated channels

Chun-Tian Xu¹•Jian-Chao Chen¹•Yi-Fan Wei¹•Han Han²•Xu Zong³•Ye Yuan³

Abstract

The transverse bowing greatly affects accuracy of the roll forming asymmetric corrugated channels (ACC). In order to control this defect, the paper first elucidates its mechanism of the production. Then the transverse bowing is explored by finite element method (FEM) using ABAQUS 2016 software and the effects of the forming parameters are analyzed. Also, a linear regression model is built using Minitab 19 software to evaluate their effects, of which standard values are measured by Pareto chart. It is observed that the number of forming channels has the greatest effect, followed by the roll gap and bending angle, and the friction coefficient has the least. Finally, to decrease the transverse bowing defect (TBD), the dominant forming parameters are optimized according to the evaluation results and the operating conditions. And the results of simulation and optimization are verified by experiments, respectively. This research shows that the TBD can be greatly controlled by the optimization of three dominant forming parameters including the roll gap, bending angle and inter-station distance for given ACC.

Keywords Asymmetric corrugated channels • Transverse bowing defect • Cold roll forming • Simulation • Parameter effect

✉ Chun-Tian Xu
xuchuntian@163.com

¹ School of Mechanical Engineering and Automation, University of Science and Technology LiaoNing, AnShan, LiaoNing, China

² School of Computer Science and Engineering, Southern University of Science and Technology, ShenZhen, GuangDong, China

³ Angang Steel Co. LTD, Anshan Iron & Steel, AnShan, LiaoNing, China

1 Introduction

Cold roll forming is a continuous metal forming process with high efficiency and precision for manufacturing strip profiles with constant cross section. The roll formed sheet products have been widely used in the construction industry, such as roofing, wall cladding, concrete form-work, and fencing. The asymmetric corrugated channels (ACC) under study, as this type of product, are mainly for fabricating the aluminum sleeves. Compared with traditional competitive paper sleeves used for the supports of such industrial roll products as aluminum coils, the aluminum ones have the advantages of low cost, high load capacity, low collapse, recyclability, and environmental protection and so on [1]. And thus, they can also be used as the supports of aluminum coils instead of paper sleeves and have wider promotion value and market development prospect, see **Fig. 1**

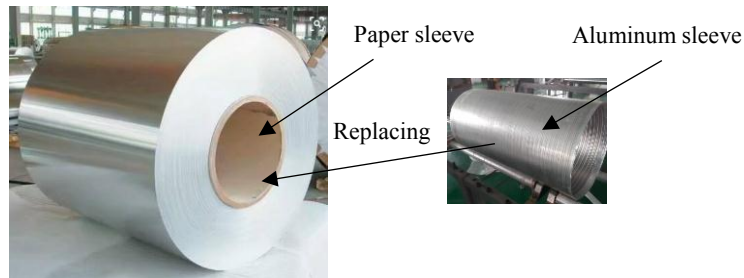


Fig.1 Aluminum coil support

However, the desired accuracy of ACC is difficult to guaranteed due to the defects like twisting and bowing in roll forming process, which inevitably affects the quality of aluminum sleeves. It has been regarded that the springback or the elastic recovery causes those above defects. For this reason, some scholars have carried out a series of studies to control these defects. Liu et al. combined experimental and numerical simulations to investigate the phenomenon of local thinning in complex sections. The results showed that the loading pattern and roll diameter had a significant effect on this defect [2]. To analyze the effect of forming parameters on the rolled product quality, Abeyrathna et al. studied three types of AHSS and UHSS steels, respectively, and found that the bowing defect was highly influenced by the flange length, material yield strength and the material strain hardening [3]. Murugesan et al. studied the longitudinal bending and springback phenomenon of Al alloy with U-profile with digital image technology and finite element method. The results show that the longitudinal strain has an effect on the geometry and the springback phenomenon only appears at the end of the profile [4]. Bidabadi et al. investigated the longitudinal bowing defect in pre-notched channel products, and the geometric and process parameters affecting this defect were respectively evaluated using Minitab software [5]. With respect to the thickness reduction in the bending zone in free U-bending, Qian et al. explored the influence of three main factors with numerical simulation and experimental through three different loading modes [6]. Based on a wide profile section, Mohammdi et al. researched the mechanism of edge wrinkling phenomenon and analyzed the effect of some forming parameters on this defect [7]. Cha and Kim found that the twisting and bowing behaviors of asymmetric channel section were most likely due to the inconsistent longitudinal strain in the web zone and flange region of the section. And the defect was significantly improved by applying a compression force in the web thickness direction after the sheet passed the final pass [8]. Tehrani et al. performed a study on the symmetrical channel section with local edge buckling phenomenon and analyzed the effect of the incremental bending angle of the adjacent roll stations on this defect [9]. Zeng et al. optimized the design of each station using the response surface method

and found that the optimized roll diameter and forming angle increment were effective in avoiding the U-channel edge wave phenomenon, and the springback was also controlled to a minimum value [10]. To control the springback of high-strength steels with cap sections, Jiao-Jiao et al. proposed an umbrella angle adjustment method in combination with angle compensation [11]. Wiebenga et al. performed robust optimization of the cold roll forming process to compensate for product defects, of which effectiveness was proved by both experimental and numerical results [12]. A parametric study of the product forming quality was performed by Bui and Ponthot, which proved that the material yield strength had a remarkable influence on the springback, while the roll station distance affect little [13].

In general, the interests of cold roll forming defects so far have mainly focused on the single U- or V-shaped section. Due to the small number of channels, the defects mainly occur in the longitudinal direction, and thus the research on the defects in transverse direction is rarely involved. Especially for the corrugated ones under study, the roll force exerted on each channel is unequal due to asymmetric channel width, which makes the transverse bowing defect (TBD) occur easily. Therefore, in view of the TBD of ACC, this study first elucidates its mechanism of the production in Sect. 2. Then the finite element model, TBD and non-uniform springback simulation are presented in Sect. 3. The effects of forming parameters are discussed in Sect. 4. The influence evaluation and optimization of forming parameters, and experimental verification are completed in Sect. 5. Finally, some valuable conclusions on how to control the TBD are provided in Sect. 6.

2 Transverse bowing mechanism of ACC

Different from longitudinal defect, the TBD usually occurs in the cross section of the roll formed product and is caused mainly by transverse non-uniform springback. As shown in **Fig. 2** (a), a large amount of bending deformation of the sheet is required to move the flat part in roll forming single channel. Naturally, the transverse tension is produced considerably due to transverse stretching at the corners of the section, which can easily lead to the corner thinning or tearing under the roll force.

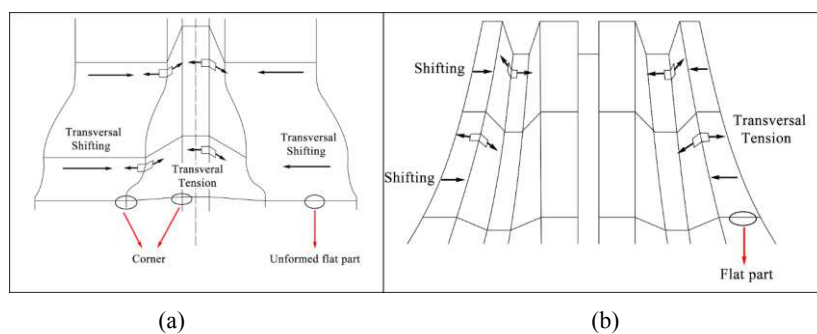


Fig. 2 Transversal tension distribution in (a) Single channel and (b) Corrugated channels

But for the roll forming ACC, since the flat part is reduced relatively, the channels on both sides require less transverse tension when being pulled toward the center, see **Fig. 2** (b). Correspondingly, the transverse tension at the corners is significantly reduced. When a final product is rolled into shape, the tension strain at the corners is variability for their asymmetrical channel width, where the middle channel is greater than two sides. This means that the springback of the sheet middle area is smaller and the transverse non-uniform springback inevitably appears, which thus makes the product TBD. And the greater the transverse non-uniform springback, the more significant the TBD of ACC.

3 Methodology

3.1 Forming sequence and geometric model

The roll forming technology of ACC adopts sequential forming method, with the middle channels formed first and next the two sides. Here the whole forming process can be divided into four groups, as shown in Fig. 3(a). Unlike V- or U-shaped single channel, the ACC can be regarded as the composition of multiple cap sections, including both narrow and wide channels, and symmetrically distributed on both sides of middle channel. Their geometric characteristics and dimensions are shown in Fig. 3(b) and Table 1, respectively.

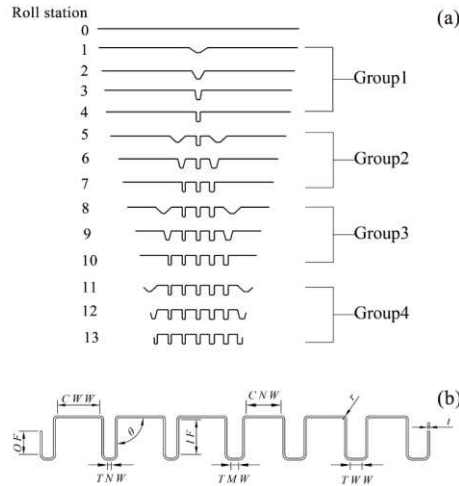


Fig. 3 Forming sequence and geometric characteristics of asymmetric corrugated channels (a) Forming sequence (b) Geometric characteristics

Table 1 Geometric dimensions

Symbols	Areas	Dimension
OF	Outer flange	2.5 mm
CWW	Wave crest wide channel web area	5.5 mm
TNW	Wave trough narrow channel web area	0.5 mm
θ	Final forming angle	90°
IF	Inner flange	4.5 mm
TMW	Wave trough middle channel web area	1 mm
CNW	Wave crest narrow channel web area	4.5 mm
r	Corner radius	0.5 mm
TWW	Wave trough wide channel web area	1.5 mm
t	Thickness	0.25 mm

3.2 Numerical simulation

3.2.1 Finite element model

This section is carried out by numerical simulation of the cold roll forming process and springback of the ACC using ABAQUS 2016 software. The built finite element model is shown in Fig. 4, which mainly consists of sheet material and 13 roll stations. The aluminum sheet is 110 mm x 550 mm, of which mechanical properties are shown in Table 2. In the roll forming simulation, the sheet forming is considered as a quasi-static process due to the lower sheet feeding. Thus, the roll deformation can

be neglected and treated as an analytic rigid body in the software [14]. Meanwhile, to improve calculation efficiency, the forming line velocity is set to 3 m/s between roll station distance 300 mm, the sheet is divided into 30360 elements using a thin shell mesh (S4R) of size 0.5 mm x 4 mm, and 5 integration points are used in the thickness direction of each element. Moreover, to better simulate the actual production with lubrication conditions, the Coulomb's friction law is adopted and the friction coefficient between sheet and roll is 0.1, as suggested by Paralikas et al. [15].

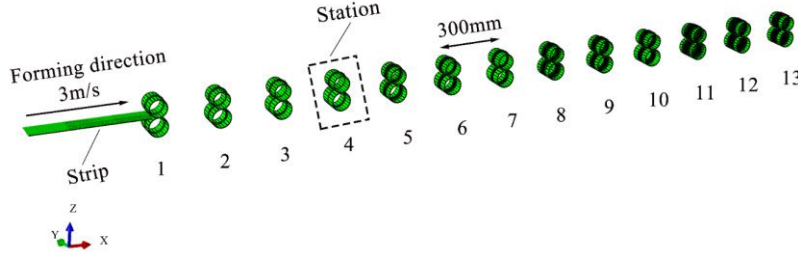


Fig. 4 Finite element model

Table 2 Material mechanical properties parameters

Parameters	Units	Values
Yield strength	MPa	275
Density	kg/m ³	2700
Ultimate tensile strength	MPa	355.8
Poisson's ratio	-	0.33
Young's modulus	MPa	69000

Due to the asymmetric characteristic of the channel width, the simulation cannot be performed only by taking half of the ACC as the case of the single channel, which results in the addition of more boundary conditions. In order to eliminate the effect of excessive friction because of roll speed difference, the lower roll is kept as the driving and the upper one is as the driven [16]. And only URY degrees of freedom are retained for the upper and lower rolls during the forming process. With respect to the sheet, to avoid its end curling forward and deviation from the forming direction, only the URY and URZ degrees of freedom are restricted. During this period, all the degrees of freedom of the intermediate nodes of the profile are constrained, while the other regions of freedom are consistent with the description above. Then the elastic recovery of the profile is analyzed based on the state at the end of quasi-static forming of the sheet.

3.2.2 Transverse bowing defect and non-uniform springback

According to **Fig. 5**, the TBD can be represented by the maximum angle θ at which the crest web deviates from the horizontal direction. Given that the angles θ_1 and θ_4 are always larger than θ_2 and θ_3 , and the size of the transverse bowing defect is measured only by the sum of θ_1 and θ_4 from the horizontal direction of the outermost two wave crest webs. Thus, θ can be calculated by Eq. (1):

$$\theta = \tan^{-1} \left(\frac{\Delta Z}{\Delta Y} \right) \quad (1)$$

where ΔZ denotes the displacement difference between the two ends of the wave web along the Z-axis direction and ΔY is the displacement difference along the Y-axis direction.

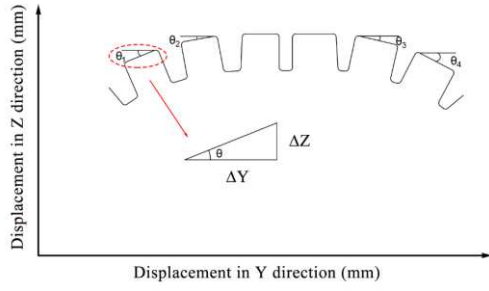


Fig. 5 Determination of transverse bowing defect

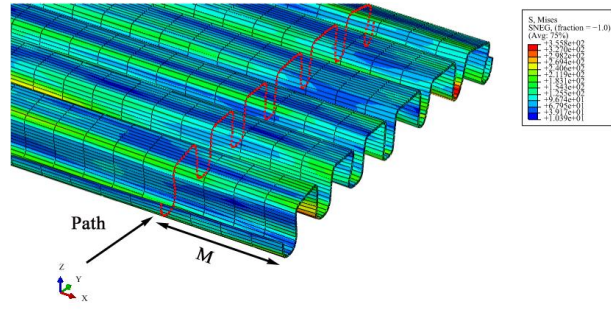


Fig. 6 Measurement path of transverse bowing defect

In order to improve the measurement accuracy of TBD, the present and after studies take the cross section of sheet after springback as the measurement path, which is M ($M=20\text{mm}$) from the sheet head, see **Fig. 6**. The corresponding transverse strain is illustrated in **Fig. 7**. As can be seen that the transverse tensile strain is not uniformly distributed in the width direction of ACC. There is a significant difference in the tensile strain at the bend of each channel. The tensile strain at the bending zone of both lateral channels is significantly smaller than that of the middle channel. And the strain on the left side is larger than that on the right side because of its asymmetric the channel width. This leads to the non-uniform springback of ACC and their bowing defect inevitably occurs, which is consistent with the transverse bowing mechanism of ACC above, as shown in **Fig. 8**.

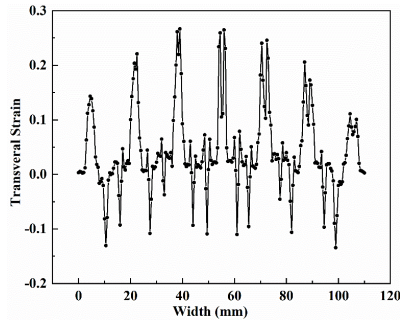


Fig. 7 Transverse strain distribution in the width direction

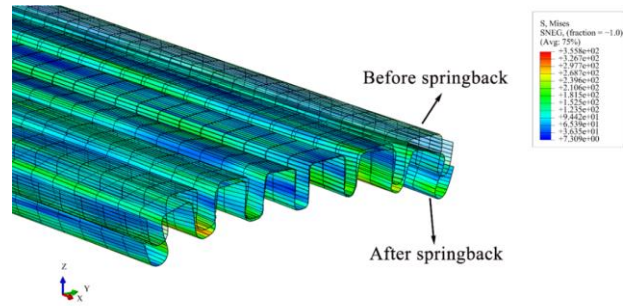


Fig. 8 Transverse non-uniform springback

4 Results and discussion

4.1 Forming parameters

The stress strain behavior of ACC is very complex under roll force [1], which leads to the types of the defects and their influencing factors very complicated, correspondingly. Here the simulations are performed for forming variables only including the friction coefficient, inter-station distance, bending angle, roll gap and number of forming channels. The simulation and after test values of the variables are provided in **Table 3**.

Table 3 Summary of forming variables and test values

Forming variables	Symbol	Quantities
Friction coefficient	FC	0.1, 0.15, 0.2
Bending angle cases	BAC	1, 2, 3
Inter-station distance (mm)	ID	300, 350, 400
Roll gap (mm)	RG	0.25, 0.5, 0.75
Number of forming channels	N	3, 5, 7

4.2 Effects of forming parameters

4.2.1 Friction coefficient

In cold roll forming process, the friction is principally used to transmit the roll driving force to the sheet metal. In order to explore its effect on the TBD, the friction coefficient between the sheet and roll is set as 0.1, 0.15 and 0.2 in simulation, respectively, according to the suggestion in literature [17]. The transverse bowing defects caused by springback under different friction coefficients are shown in Fig. 9(a). Different from single channel, although there exists sliding arc surface between the roll and the sheet in roll forming, it is seen that the TBD does not change significantly with the friction coefficient, which means that the friction coefficient between the roll and sheet has little effect. However, to improve the surface smoothness of the product and decrease sheet tearing, the friction coefficient should be as small as possible by adding lubricating oil in the actual production.

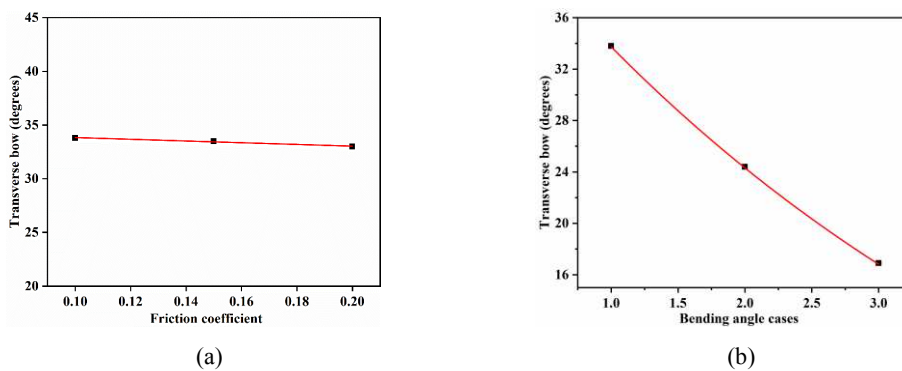


Fig. 9 Friction coefficient (a) and bending angle (b) influence on transverse bowing defect

4.2.2 Bending angle

Since the TBD is not obvious in the middle region of ACC, see Fig. 8, here the effects of the bending angles only consider groups 2, 3 and 4. Correspondingly, the forming cases of Table 4 are used for the research. The transverse bowing defects under different bending angles of three cases are shown in Fig. 9(b) by simulation.

Table 4 Bending angle strategy

Group	Passes	Case 1	Case 2	Case 3
1	1	33	33	33
	2	60	60	60
	3	81	81	81
	4	90	90	90
2	5	43	50	57
	6	75	75	75
	7	90	90	90
3	8	43	50	57
	9	75	75	75
	10	90	90	90
4	11	43	50	57
	12	75	75	75
	13	90	90	90

As can be seen that the TBD of case 3 is dropped by 50% compared to case 1. This indicates that increasing the forming angle of the first pass of groups 2, 3 and 4 can effectively ameliorate the bowing phenomenon. However, the maximum peak strain of the ACC becomes large with the bending angle, which enlarges the risk of profile fracture [1].

4.2.3 Inter-station distance

The determination of the inter-station distance needs to define the length of sheet deformation zone between two passes. Based on the study of Bhattacharyya et al. [18], the minimum deformation zone length (L) can be calculated by Eq. (2):

$$L = \sqrt{\frac{8a\Delta\theta^3}{3t}} \quad (2)$$

where a is sheet flange length and $\Delta\theta$, t are forming angle increment and material thickness, respectively.

To investigate the effect of inter-station distance, distances 300, 350 and 400 mm are taken for consideration in this section, respectively, as shown in Fig. 10(a). It is seen that the transverse bowing defect decreases obviously with the increase of roll station distance. In other words, increasing the roll station distance can reduce the springback to a certain extent, which conforms to the results of previous numerical studies by Park and Anh [19]. However, enlarging the roll station distance also means that the roll forming device will take up more space and increase its cost.

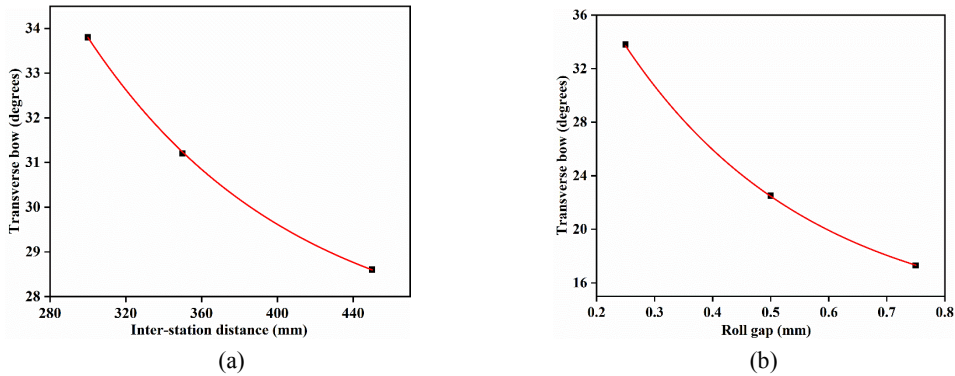


Fig. 10 Inter-station distance (a) and roll gap (b) effects on transverse bowing defect

4.2.4 Roll gap

Roll gap is regarded as an important process parameter in the assembly of cold roll forming machine, of which value has a significant impact on the quality of the final product. According to sheet width, roll gaps 0.3, 0.5 and 0.75 mm are used for simulation, respectively. As shown in Fig. 10(b) that the TBD of the ACC can be significantly improved by enlarging roll gap. This indicates that the transverse non-uniform springback decreases. Surprisingly, however, the simulation result contradicts the conclusion of the previous research by Wiebenga et al. [12]. This is mainly because the previous study is limited to the single channel, of which springback becomes larger with the roll gap. But with respect to the multi-channel springback, larger roll gap can effectively decrease the tension strain inhomogeneity between channels and their mutual interference in roll forming, and thus, their non-uniform springback is naturally improved.

It must be noted that the roll forming aluminum sheet, as a kind of soft material is more sensitive to the roll gap than the steel. Although the TBD of roll gap 0.75 mm ($3t$) is reduced by about 48.8% and 33.4% compared to those of roll gaps 0.25 mm (t) and 0.5 mm ($2t$), the dimensional accuracy

of both the bending angle zone and web region of the formed section is greatly affected, and even a large error is produced. Conversely, if the dimensional accuracy is guaranteed under the roll gap 0.25mm (t), it not only increases the difficulty of roll forming device assembly, but also the ACC are prone to fracture failure in the bending region during the forming process. Therefore, the roll gap 0.5 mm ($2t$) becomes the best choice of three gaps.

4.2.5 Number of forming channels

In order to analyze the effect of forming channels on the transverse bowing, the number of forming channels 3, 5 and 7 are used to investigate, respectively, and the corresponding roll flower patterns are shown in **Fig. 11**. Unexpectedly, the TBD of the product varies noticeably with the increase of the number of forming channels, as shown in **Fig. 12(a)**. It is calculated that the TBD of the number of forming channels 7 increases by about 74.6% relative to channels 3. This is mainly because the increase of the number of forming channels enlarges the non-uniformity transverse springback of the product, correspondingly. The springback difference is more obvious between the edge area and middle zone of the corrugated channels 7 especially under the asymmetric roll force, which easily causes both sides tearing, as shown in **Fig. 12(b)**.

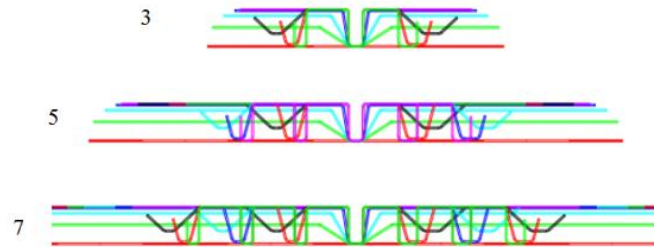
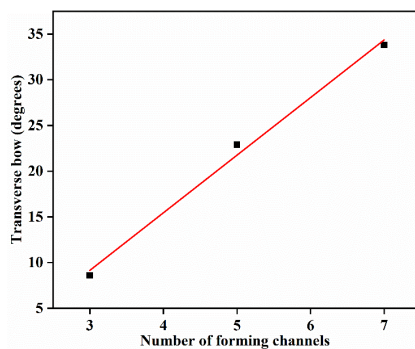
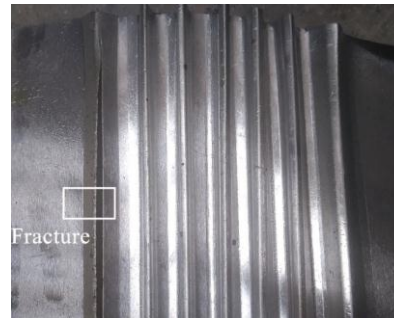


Fig. 11 Roll flower patterns



(a)



(b)

Fig. 12 Number of forming channels effects

5 Experimental verification

5.1 Experimental setup

The cold roll forming experimental setup for ACC mainly composed of stations, uncoiler, motor and control box, see **Fig. 13**. The sheet is first unwound by the uncoiler, then passes through each station in succession until the final product is formed. And the inverter motor provides the driving force for the lower rolls during this process.

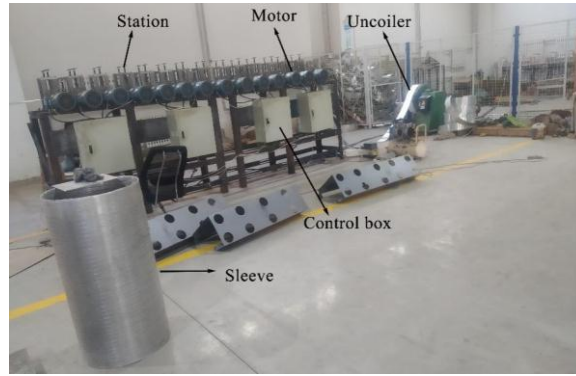


Fig. 13 Cold roll forming line

5.2 Verification of Simulation Results

In order to further verify the reliability of the FEM results, the simulation data by FEM and experimental results of the transverse bowing of ACC under the initial operation conditions (see **Table 5**) are compared. In addition, the relative error can be defined by **Eq. (3)** :

$$e = \frac{|D_f - D_e|}{D_e} \quad (3)$$

where e represents the relative error, D_f means the simulation data, and D_e represents the experimental results.

Table 5 Initial operation conditions

Parameters	Value
Initial strip width (mm)	110
Inter-station distance (mm)	300
Bending angle (degrees)	33,60,81,90;43,75,90;43,75,90;43,75,90
Roll gap (mm)	0.25

As shown in **Fig. 14**, relative error e of transverse bowing is within the allowable range of 5%. This may be caused by the assembly error of the experimental device. For example, the roll gap is adjusted greater than sheet width 0.25 mm for avoiding sheet tearing in the experiment, which results in smaller flange height and springback, correspondingly. Therefore, the built FEM in **Fig. 4** can be used for research of TBD.

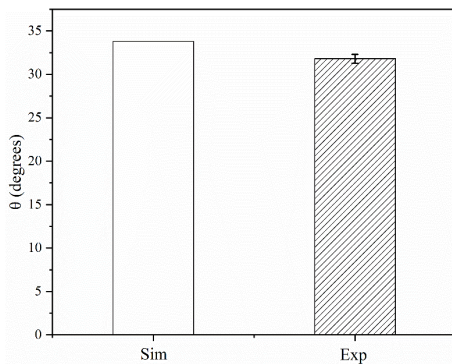


Fig. 14 Validation of FEM results

5.3 Regression analysis

In order to further measure the effects of above forming parameters on TBD, a linear regression

analysis is performed in this section using Minitab 19 software. And the regression equation can be expressed as Eq. (4).

$$\theta=22.34-0.5FC-0.0465ID-34.34RG+5.992N-8.364BAC \quad (4)$$

where the values of FC , ID , RG , N and BAC are shown in Table 3.

Table 6 shows the results evaluated by Eq. (4). Where P represents the influence degree of each forming parameter; T denotes the positive or negative correlation between the impacts of influencing parameters on the defect. It can be seen that the value of R-Square is 98.51%, which implies the high accuracy of the fitting curve. And thus, Eq. (4) can be used to evaluate the effects of forming parameters on TBD. When the P is greater than 0.05, the effect of parameter is negligible. And the smaller the P , the greater the impact on the defect. While the larger the absolute value of T , the greater the effect.

Table 6 Evaluation results of forming parameters

Term	Coef	SE Coef	T-value	P-value
Constant	22.34	6.78	3.3	0.022
FC	-0.5	17.5	-0.03	0.979
ID	-0.0465	0.0175	-2.66	0.045
RG	-34.34	3.5	-9.82	0.000
N	5.992	0.437	13.71	0.000
BAC	-8.364	0.874	-9.57	0.000

S=1.41794, R-Sq=98.51%, R-Sq(adj)=97.01%

To evaluate above forming parameters on the transverse bowing more accurately, their standardized effects are measured by Pareto chart in Fig 15. It can be seen that the standardized effect of the number of forming channel is largest, which is 13.71, while the effect of the friction coefficient is the smallest, which is near -2.66. Again, it further illustrates that the number of forming channels has prominent influence on the TBD, followed by roll gas, bending angle and inter-station distance, while the impact of friction coefficient is negligible, as agrees with the studies by Bidabadi et al. [20].

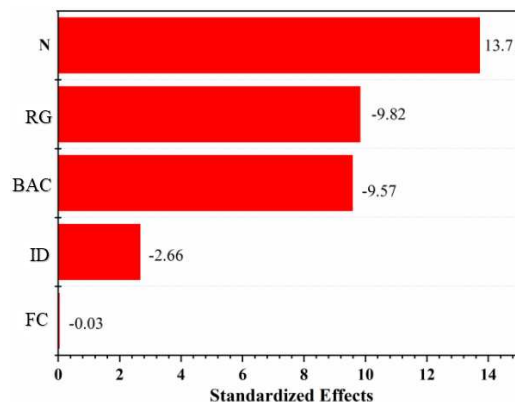


Fig 15 Pareto chart of standardized effects

5. 4 Optimization of dominant forming parameters

Based on the evaluation results of the regression model, the transverse bowing of ACC is affected by the forming parameters of number of channels, roll gap, bending angle and inter-station distance. Thus, to improve the TBD, the dominant forming parameters are optimized under the given number 7 of forming channel. Here the optimized bending angle case is adjusted from 1 to 3, the roll gap is

corrected from 0.25 to 0.5 mm, and the inter-station distance is expanded from 300 to 400 mm. **Fig. 16** shows the profile of roll forming asymmetric corrugated channels before and after parameter optimization. It can be seen that the quality of product has been significantly improved after parameter optimization.

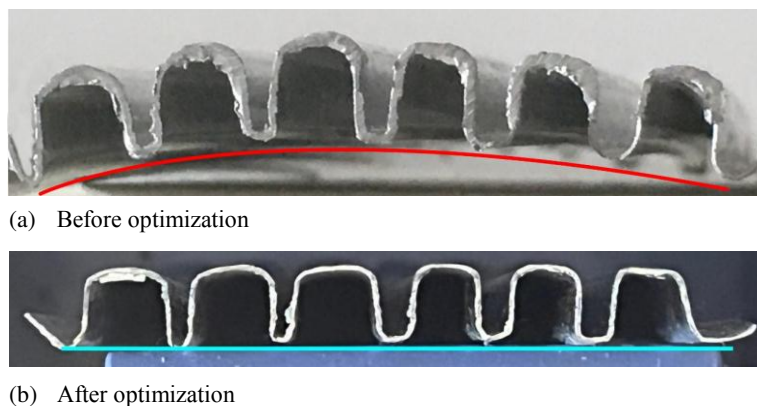


Fig. 16 Asymmetric corrugated channels

In addition, by calculation, the optimized θ decreases by about 88.5%, 89.9%, and 89.8% compared to the initial value for simulation, experiment, and regression prediction, respectively. And their relative errors are both within 10%, as shown in **Fig. 17**. This not only proves the reliability of the regression model, but also indicates that the TBD can be controlled by optimizing the dominant forming parameters.

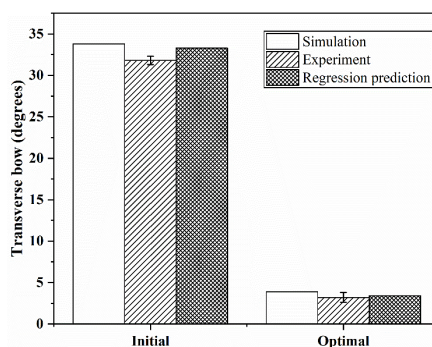


Fig. 17 Transverse bow comparison

6 Conclusions

(1) The transverse bowing defect of ACC arises from non-uniform springback in the transverse direction after sheet unloading by analyzing its mechanism of production.

(2) Different from single channel, the transverse springback of ACC decreases with the roll gap, mainly because its non-uniformity is improved with the number of channels and roll gap.

(3) Evaluated by linear regression equation, the number of forming channels has a significant effect on the transverse bowing defect of ACC, followed by the roll gap, bending angle and inter-station distance, and the friction coefficient has the least.

(4) For given ACC, the transverse bowing defect can be controlled by the optimization of dominant forming parameters of roll gap, bending angle, and inter-station distance.

Funding

This Project is supported by programs for Natural Science Foundation of Liaoning Province (2019-ZD-0275) and Intelligent Industry of Anshan Iron and Steel Corporation (2020-KD-1001).

References

1. Xu C, Wei Y, Pan T, Chen J (2021) A study of cold roll forming technology and peak strain behavior of asymmetric corrugated channels. *The International Journal of Advanced Manufacturing Technology* 118(11-12): 4213-4223
2. Liu XL, Cao JG, Chai XT, He ZL, Liu J, Zhao RG (2017) Experimental and numerical prediction of the local thickness reduction defect of complex cross-sectional steel in cold roll forming. *The International Journal of Advanced Manufacturing Technology* 95(11):1837-1848
3. Abeyrathna B, Rolfe B, Weiss M (2017) The effect of process and geometric parameters on longitudinal edge strain and product defects in cold roll forming. *The International Journal of Advanced Manufacturing Technology* 92(1):743-754
4. Murugesan M, Sajjad M, et al (2021) Experimental and Numerical Investigation of AA5052-H32 Al Alloy with U-Profile in Cold Roll Forming. *Materials* 14(2):470-489
5. Bidabadi BS, Naeini HM, Tafti RA, Barghikar H (2016) Experimental study of bowing defects in pre-notched channel section products in the cold roll forming process. *The International Journal of Advanced Manufacturing Technology* 87(3): 997-1011
6. Qian Z, Zhao Y, Wang C, et al (2021) Numerical and Experimental Investigation of the Bending Zone in Free U-Bending. *Journal of Manufacturing Science and Engineering* 143(9):1-32
7. Mohammadi NH, Moslemi NH, Safdarian R, Kasaei MM, Akbari D, Abbaszadeh B (2018) Effect of forming parameters on edge wrinkling in cold roll forming of wide profiles. *The International Journal of Advanced Manufacturing Technology* 101(1): 181-194
8. Cha WG, Kim N (2013) Study on twisting and bowing of roll formed products made of high strength steel. *International Journal of Precision Engineering and Manufacturing* 14(9): 1527-1533
9. Tehrani MS, Hartley P, Naeini HM, Khademizadeh H (2006) Localised edge buckling in cold roll-forming of symmetric channel section. *Thin-Walled Structures* 44(1): 184-196
10. Zeng G, Li SH, Yu ZQ, Lai XM (2009) Optimization design of roll profiles for cold roll forming based on response surface method. *Materials & Design*(2009): 30(6): 1930-1938
11. Jiao-Jiao C, Jian-Guo C, Qiu-Fang Z, Jiang L, Ning Y, Rong-guo Z (2020) A novel approach to springback control of high-strength steel in cold roll forming. *The International Journal of Advanced Manufacturing Technology* 107(1): 1793-1804
12. Wiebenga JH, Weiss M, Rolfe B, van den Boogaard AH (2013) Product defect compensation by robust optimization of a cold roll forming process. *Journal of Materials Processing Technology* 213(6): 978-986
13. Bui QV, Ponthot JP (2008) Numerical simulation of cold roll-forming processes. *Journal of Materials Processing Technology* 202(1-3): 275-282
14. Rossi B, Degée H, Boman R (2013) Numerical simulation of the roll forming of thin-walled sections and evaluation of corner strength enhancement. *Finite Elements in Analysis and Design* 72(9): 13-20
15. Paralikas J, Salonitis K, Chryssolouris G (2008) Investigation of the effects of main roll-forming process parameters on quality for a V-section profile from AHSS. *The International Journal of Advanced Manufacturing Technology* 44(1): 223-237
16. Li ZX, Shu XD, Yin AM, Guo DL (2018) Experimental and numerical analysis on the forming and shearing quality of C-channel steel. *The International Journal of Advanced Manufacturing Technology* 94(9): 3665-3678
17. Safdarian R, Moslemi Naeini H (2015) The effects of forming parameters on the cold roll forming of

- channel section. *Thin-Walled Structures* 92(3): 130-136
18. Bhattacharyya D, Smith P, Yee C, Collins I (1984) The prediction of deformation length in cold roll-forming. *Journal of Mechanical Working Technology* 9(2):181-191
 19. Park H, Anh T (2010) Finite element analysis of roll forming process of aluminum automotive component. *International Forum on Strategic Technology* 2010:5-9
 20. Bidabadi BS, Naeini HM, Tehrani MS, Barghikar H (2016) Experimental and numerical study of bowing defects in cold roll-formed U-channel sections. *Journal of Constructional Steel Research* 118(3): 243-253

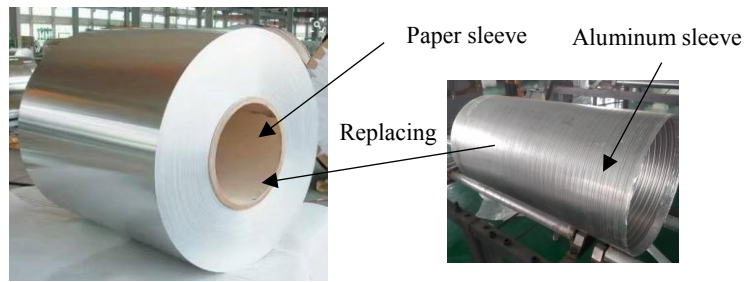


Fig.1 Aluminum coil support

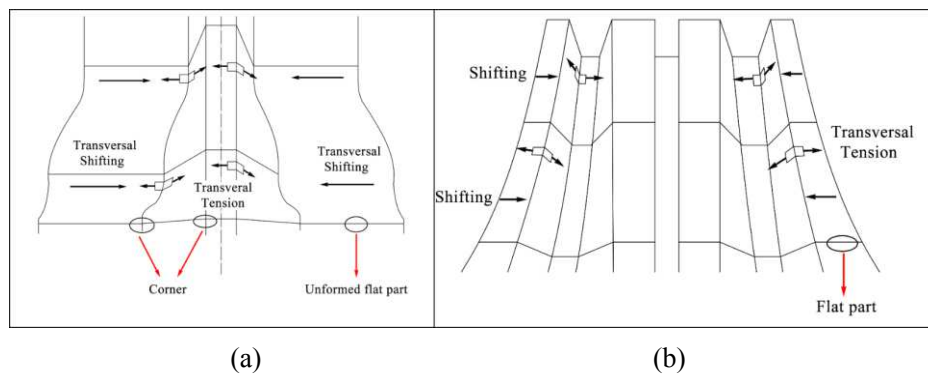


Fig. 2 Transversal tension distribution in (a) Single-channel and (b) Corrugated channels

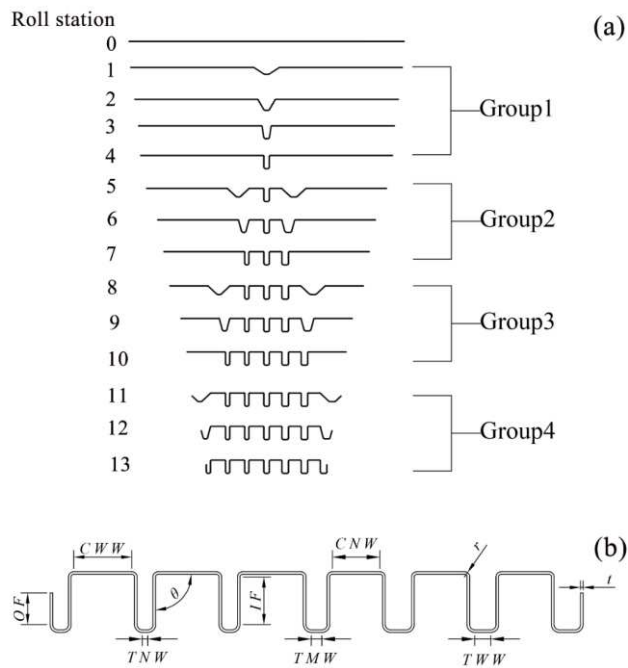


Fig. 3 Forming sequence and geometric characteristics of asymmetric corrugated channels (a) Forming sequence (b) Geometric characteristics

Table 4 Geometric dimensions

Symbols	Areas	Dimension
OF	Outer flange	2.5 mm
CWW	Wave crest wide groove web area	5.5 mm
TNW	Wave trough narrow groove web area	0.5 mm
θ	Final forming angle	90°
IF	Inner flange	4.5 mm
TMW	Wave trough middle groove web area	1 mm
CNW	Wave crest narrow groove web area	4.5 mm
r	Corner radius	0.5 mm
TWW	Wave trough wide groove web area	1.5 mm
t	Thickness	0.25 mm

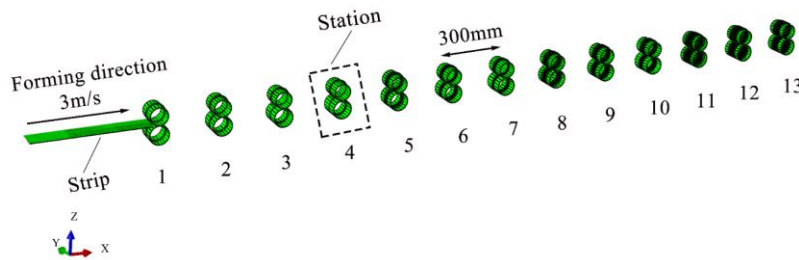


Fig. 4 Finite element model

Table 5 Material mechanical properties parameters

Parameters	Units	Values
Yield strength	MPa	275
Density	kg/m ³	2700
Ultimate tensile strength	MPa	355.8
Poisson's ratio	-	0.33
Young's modulus	MPa	69000

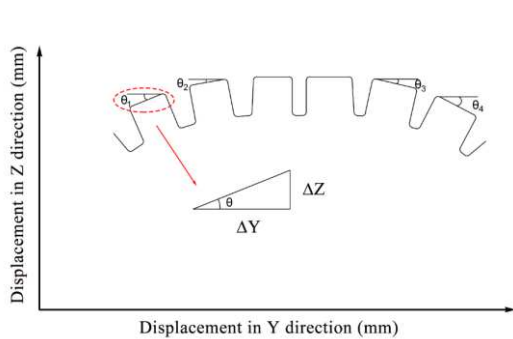


Fig. 5 Determination of transverse bowing defect

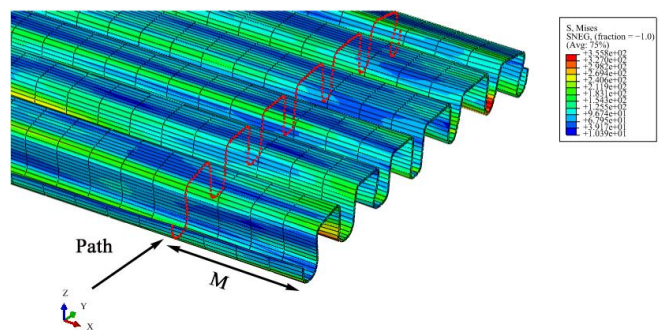


Fig. 6 Measurement path of transverse bowing defect

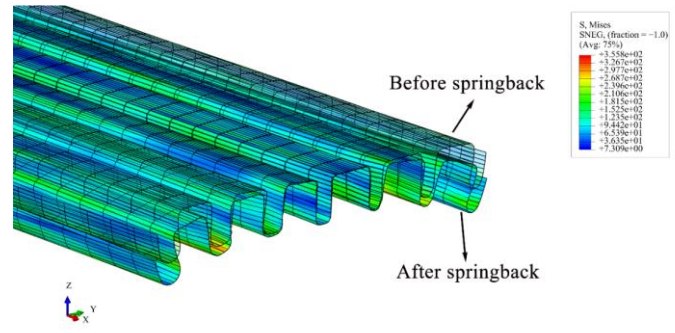
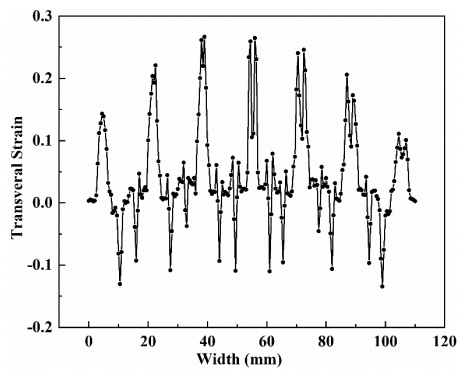
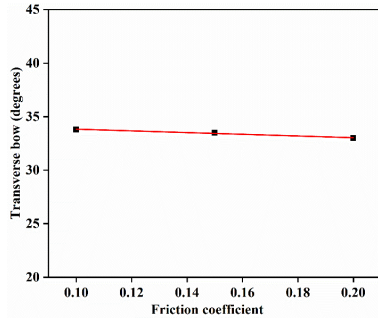


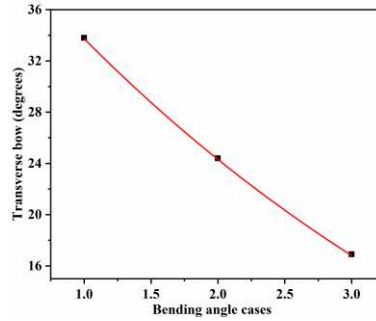
Fig. 7 Transverse strain distribution in the width direction **Fig. 8** Transverse non-uniform spring back

Table 6 Summary of forming variables and test values

Forming variables	Symbol	Quantities
Friction coefficient	FC	0.1, 0.15, 0.2
Bending angle cases	BAC	1, 2, 3, 4
Inter-station distance (mm)	ID	300, 350, 400
Roll gap (mm)	RG	0.25, 0.375, 0.5
Number of forming channels	N	3, 5, 7



(a)



(b)

Fig. 9 Friction coefficient (a) and bending angle (b) influence on transverse bowing defect

Table 7 Bending angle strategy

Group	Passes	Case 1	Case 2	Case 3
1	1	33	33	33
	2	60	60	60
	3	81	81	81
	4	90	90	90
2	5	43	50	57
	6	75	75	75
	7	90	90	90
3	8	43	50	57
	9	75	75	75
	10	90	90	90
4	11	43	50	57
	12	75	75	75
	13	90	90	90

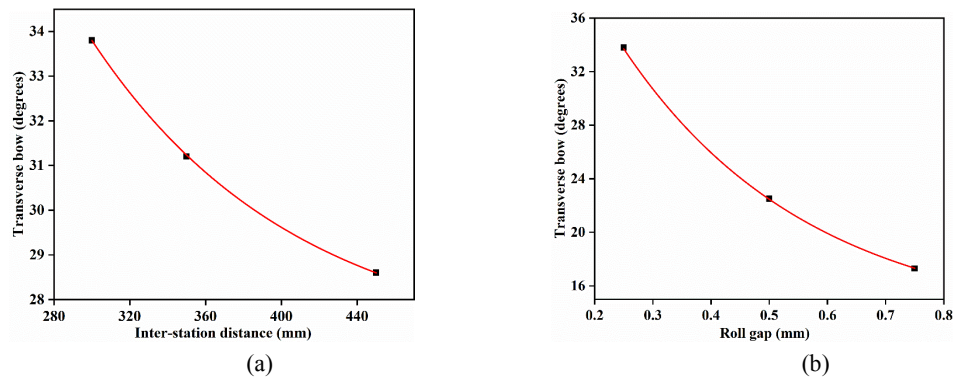


Fig. 10 Inter-station distance (a) and roll gap (b) effects on transverse bowing defect

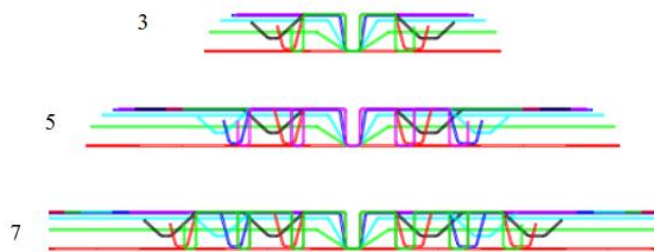
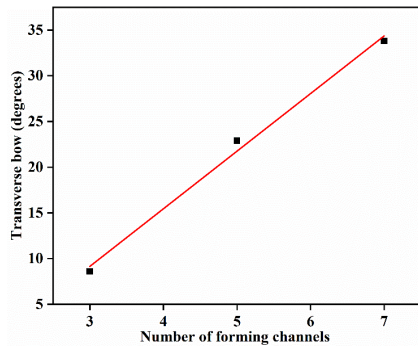


Fig. 11 Roll flower patterns



(a)



(b)

Fig. 12 Number of forming channels effects

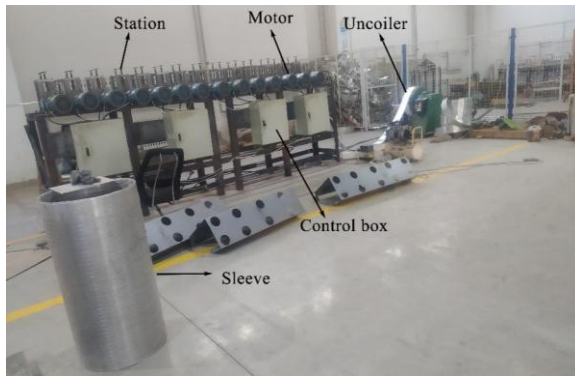


Fig. 13 Cold roll forming line

Table 8 Initial operation conditions

Parameters	Value
Initial strip width (mm)	110
Inter-station distance (mm)	300
Bending angle (degrees)	33,60,81,90;43,75,90;43,75,90;43,75,90
Roll gap (mm)	0.25

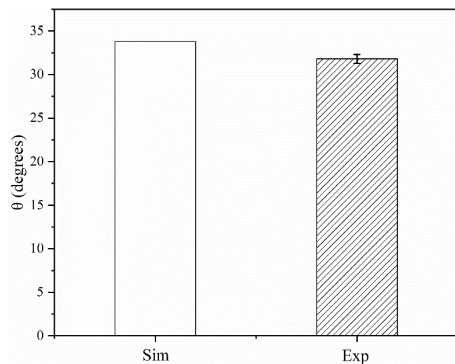


Fig. 14 Validation of FEM results

Table 6 Evaluation results of forming parameters

Term	Coef	SE Coef	T-value	P-value
Constant	22.34	6.78	3.3	0.022
FC	-0.5	17.5	-0.03	0.979
ID	-0.0465	0.0175	-2.66	0.045
RG	-34.34	3.5	-9.82	0.000
N	5.992	0.437	13.71	0.000
BAC	-8.364	0.874	-9.57	0.000

S=1.41794, R-Sq=98.51%, R-Sq(adj)=97.01%

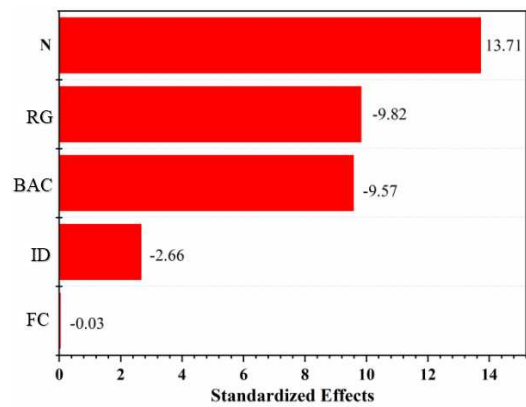
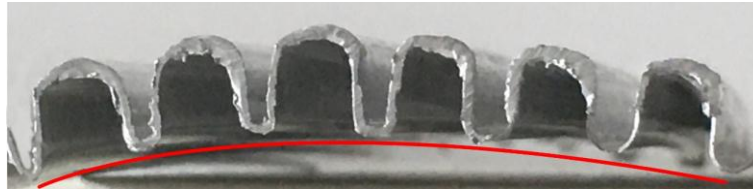


Fig. 15 Pareto chart of standardized effects



(a) Before optimization



(a) After optimization

Fig. 16 Asymmetric corrugated channels

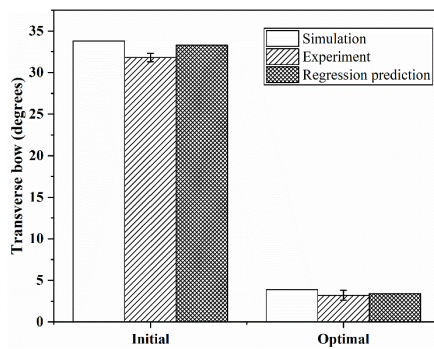


Fig. 17 Transverse bow comparison